

Spin-flip scattering near the metal-to-insulator transition in $\text{Cd}_{0.95}\text{Mn}_{0.05}\text{Se:In}$

T. Dietl and M. Sawicki

Institute of Physics, Polish Academy of Sciences, Al. Lotnikow 32/46, PL-02668 Warsaw, Poland

M. Dahl and D. Heiman

Francis Bitter National Magnet Laboratory, Massachusetts Institute of Technology, Cambridge, Massachusetts 02139

E. D. Isaacs

AT&T Bell Laboratories, Murray Hill, New Jersey 07974

M. J. Graf

Department of Physics, Boston College, Chestnut Hill, Massachusetts 02167

S. I. Gubarev and D. L. Alov

Institute of Solid State Physics, Academy of Sciences of the U.S.S.R., Chernogolovka, 142432 U.S.S.R.

(Received 10 September 1990)

Spin dynamics of electrons in n -type $\text{Cd}_{0.95}\text{Mn}_{0.05}\text{Se}$ near the metal-to-insulator transition are probed by means of inelastic-light-scattering measurements as a function of magnetic field up to 8 T and temperature down to 0.25 K. The observed Raman spin-flip scattering line is demonstrated to arise from itinerant (diffusive) electrons. The spin-split energies (Stokes shifts), being determined by the s - d exchange interaction, increase strongly as the temperature is lowered, and at 0.25 K attain values that correspond to an effective Landé factor as large as 500. Variations of the spin-split energy with the magnetic field follow a modified Brillouin function suitable for this diluted magnetic semiconductor in a paramagnetic phase. A better description of experimental results is obtained, however, assuming the existence of an additional magnetization that depends only weakly on the external magnetic field. Such magnetization could be induced by bound magnetic polarons, and, therefore, its appearance points indirectly to the presence of local s spins on the metallic side of the metal-to-insulator transition. Studies of the linewidth in forward- and backscattering geometries provide information on the spin-relaxation time T_2 and spin-diffusion coefficient D_s of itinerant electrons. The magnitude of T_2 is shown to be primarily determined by (i) spin-flip scattering of electrons by magnetic ions and (ii) motionally narrowed inhomogeneous broadening caused by compositional fluctuations of magnetization. It is demonstrated that, in agreement with theoretical expectations, both T_2 and D_s are strongly affected by electron-electron interactions and localization corrections.

I. INTRODUCTION

Recent experimental studies of doped semiconductors in the vicinity of the metal-to-insulator transition (MIT)¹ have usually been analyzed in terms of a phenomenological two-fluid model.²⁻⁴ In this model the relevant electronic states are assumed to be made up of two distinct components: Fermi-liquid quasiparticles and electron local magnetic moments. The former contribute to nonzero conductivity and are thought to be correctly described by renormalization-group (RG) methods.^{1,5} A central result of the RG approach has been the demonstration that when the ratio of elastic-scattering rate to electron kinetic energy increases, the low-temperature conductivity acquires quantum corrections that result ultimately in quasiparticle localization. These corrections are determined by diffusion poles of the Fermi-liquid correlation functions. A behavior of the conductivity at criticality, as well as the position of the MI transition

point are, therefore, strongly affected by magnetic field, spin-splitting, and spin-dependent scattering as these perturbations cut off the diffusion poles in the appropriate correlation functions. The same formalism also describes a divergence of the localization length of the Fermi-liquid electrons. This length controls the hopping conductivity and dielectric susceptibility on the insulator side of the MIT. The local moments, in turn, contribute to magnetic and thermodynamic^{2,6} properties, as well as to high-frequency conductivity.⁷ Formation of local moments may involve states far in energy from the Fermi energy. Such states are outside the scope of the RG methods and, perhaps, are better handled in terms of a disordered Hubbard model.^{8,9} Because of the decoupling effect of the Hubbard repulsion and of the intersite Coulomb interaction among localized electrons,^{10,11} no charge transport is allowed between local moments and the rest of the system. However, the exchange coupling between itinerant and local electrons may increase the spin-flip scattering

efficiency, thereby affecting the low-frequency conductivity. Furthermore, one may expect a gradual conversion of quasiparticles into local moments when proceeding from the metal to the insulator. Such conversion will shrink the phase space occupied by the quasiparticles. It has been speculated¹² that a divergence of the Hall coefficient, which was found^{12,13} to occur deep in the insulating phase, reflected the disappearance of the Fermi-liquidlike states.

In this paper we report on spin-flip Raman-scattering (SFRS) experiments carried out down to 0.25 K on barely metallic $\text{Cd}_{0.95}\text{Mn}_{0.05}\text{Se}:\text{In}$ samples with electron concentration $n = 7 \times 10^{17} \text{ cm}^{-3}$.¹⁴ Measurements were carried out at the MIT National Magnet Laboratory in a top-loading dilution refrigerator equipped with optical fibers. Previous comprehensive SFRS studies^{15–17} of n -type $\text{Cd}_{0.95}\text{Mn}_{0.05}\text{Se}$ concerned material with lower net donor concentration $n \leq 10^{17} \text{ cm}^{-3}$. Such samples are well in the insulating phase, as the Mott critical concentration, estimated from the effective mass and dielectric constant of CdSe, is about $3 \times 10^{17} \text{ cm}^{-3}$. Therefore, the SFRS studies provided information on spin dynamics of electrons bound to donors, which have a Bohr radius of $\sim 38 \text{ \AA}$. It turned out that s - d exchange interaction exerted a dramatic influence on the SFRS spectrum. In particular, the spin-splitting was nonzero even in the absence of an external magnetic field. This phenomenon, known as the bound magnetic polaron (BMP), resulted from the mutual alignment of the electron spin and magnetic spins residing within the Bohr orbit of the donor.^{17–19} This spin splitting was about 0.8 meV at $T \geq 2 \text{ K}$, and increased up to 1.7 meV at $\sim 0.13 \text{ K}$, reflecting a substantial increase in the magnetic susceptibility $\chi(T)$ of Mn spins.¹⁶ The value of spin splitting increased even further under the presence of the external magnetic field, reaching about 15–20 meV when the Mn spins became fully spin polarized.¹⁷ The SFRS line was inhomogeneously broadened by thermal^{18,19} and compositional²⁰ fluctuations of the magnetization. A successful quantitative interpretation of the above results made it possible to determine the s - d exchange integral,^{18,21} as well as provide information on magnetic susceptibility of Mn spins down to 0.13 K.¹⁶ The values of $\chi(T)$ deduced in this way are in agreement with those yielded by direct millikelvin magnetic measurements.^{22,23} Since the latter were carried out for both a metallic In-doped sample ($n = 8 \times 10^{17} \text{ cm}^{-3}$)²³ and nominally undoped crystal²² (i.e., with n in the range $10^{16} - 10^{17} \text{ cm}^{-3}$), this agreement suggests that neither a Ruderman-Kittel-Kasuya-Yosida (RKKY)-type interaction nor BMP's affect substantially the total magnetic response of the system. Instead, $\chi(T)$ appears to be mostly determined by superexchange antiferromagnetic interactions which give rise to the temperature dependence specific to disordered antiferromagnets,² $\chi(T) \sim T^{-\beta}$ with $0.6 \leq \beta \leq 0.7$. This dependence holds down to $\sim 100 \text{ mK}$, where spin-glass freezing is observed.^{22,23}

Transport studies^{3,23–25} of n -type $\text{Cd}_{0.95}\text{Mn}_{0.05}\text{Se}$ have spanned a wide concentration range, $3 \times 10^{16} \text{ cm}^{-3} \leq n \leq 2 \times 10^{18} \text{ cm}^{-3}$. These studies revealed an unusual sensitivity of the conductivity on temperature and mag-

netic field. Since the corresponding effects were absent in CdSe, it has been concluded that they have been caused by the s - d interaction. In particular, the low-field positive magnetoresistance has been attributed^{3,25} to the influence of the giant s - d exchange spin-splitting on the spin-spin correlation function. Another interesting result was the observation, below $\sim 0.5 \text{ K}$, of a sudden drop of metallic conductivity in samples with $n \leq 10^{18} \text{ cm}^{-3}$.^{23,25} For $n \approx 6 \times 10^{17} \text{ cm}^{-3}$ this drop resulted in the metal-to-insulator transition when the temperature was lowered. Since near the MIT the conductivity is especially sensitive to the spin-dependent scattering, the scattering of itinerant electrons by Mn-spin fluctuations was taken into consideration. The corresponding scattering rate, however, predicted a temperature dependence and magnitude far too small to explain the data.^{23,25} It has therefore been argued,^{3,23} that regions of enhanced Mn-spin polarization around local electron magnetic moments (i.e., BMP's) constitute centers of additional spin-disorder scattering. The estimated efficiency of this scattering mode increases steeply with decreasing temperature and magnetic field, so that the calculated conductivities become in qualitative accord with the experimental results.²³ It is also possible that the low-temperature drop of conductivity reflects a temperature-dependent conversion of quasiparticles into local moments, as the binding energy of BMP's grows when the temperature is lowered. Finally, one might conjecture that the s - d coupling renormalizes quasiparticle properties by means of dynamic effects.^{3,4} This renormalization could be important for quasiparticles with energies smaller than the energy width of the Mn-spin excitation spectrum. This problem has recently been considered theoretically⁴ with the conclusion that the dynamic effects do influence the spin-spin correlation function. Whether these effects would markedly perturb the conductivity is yet to be elucidated.

It is clear from the above discussion that SFRS, if detected, constitutes a valuable tool to probe such a system, because the SFRS spectrum is directly proportional to the spin-spin correlation function.²⁶ In agreement with previous works on SFRS in metallic CdS:In (Ref. 27) and $\text{Cd}_{0.985}\text{Mn}_{0.015}\text{S}:\text{In}$,²⁸ we find in our samples the SFRS line to be diffusive and to grow linearly with the magnetic field. As argued in the following sections, such behavior indicates that the spin correlation function is that of itinerant electrons. This is just the correlation function that determines the conductivity near the MIT. Moreover, the correlation function in question involves the spin-relaxation time, which controls the degree of luminescence polarization²⁹ and the magnitude of photomagnetization³⁰ under optical pumping conditions.

The outline of this paper is as follows. In Sec. II we discuss sample characterization and experimental procedures. Section III gives experimental results and their discussion. In particular, we present the correlation function adopted to describe the data and then discuss values of spin-splittings, spin-relaxation time, and spin-diffusion coefficient deduced by a comparison of this function with the Stokes shift measured as a function of magnetic field and temperature. Finally, Sec. IV contains the main conclusions of this work.

II. EXPERIMENTAL BACKGROUND

A. Samples

The material used for this study was Bridgman-grown $\text{Cd}_{1-x}\text{Mn}_x\text{Se}:\text{In}$ with a nominal x value of 0.05 with In-donor concentration of $\sim 5 \times 10^{17} \text{ cm}^{-3}$. Four samples were cut from a single crystalline grain of volume $\sim 0.5 \text{ cm}^3$. Three samples were shaped into the Hall bars with dimensions $10 \times 2 \times 0.4 \text{ mm}^3$. The remaining sample, on which our SFRS experiments were performed, was in the form of a square plate with a thickness of $\sim 1 \text{ mm}$ and with the c axis perpendicular to the largest surface. Six electrical contacts to the Hall-bar samples were made using indium solder. The net donor concentration determined by room-temperature Hall-effect measurements on each Hall-bar sample was $n = 7 \times 10^{17} \text{ cm}^{-3}$, with scatter smaller than 8%. A systematic low-temperature resistivity study²³ of such samples indicates that the conductivity between 4.2–0.5 K is $30 (\Omega \text{ cm})^{-1}$ and then drops to about $15 (\Omega \text{ cm})^{-1}$ at 50 mK. This temperature dependence was confirmed in the course of the present optical work. Actually, a strong variation of the sample resistance at millikelvin temperatures was used to estimate the sample temperature under laser illumination in the ^3He - ^4He dilution refrigerator.

B. Experimental procedure

Spin-flip Raman scattering experiments were carried out in three different cryogenic systems for the different temperature ranges required; a ^4He flowing-gas cryostat for $T \geq 1.8 \text{ K}$, a pumped liquid ^3He cryostat for $0.4 \leq T \leq 4.2 \text{ K}$, and a top-loading dilution refrigerator for $0.1 \leq T \leq 0.8 \text{ K}$. A fiber-optic system was used to pipe light into and out of both the dilution refrigerator and ^3He cryostat. This system, described elsewhere,³¹ has in its present version one collection and two excitation fibers. The Raman-scattered light was collected along the normal sample surface over a solid angle corresponding to $f/3$ collection optics. Two excitation fibers were mounted in a way enabling illumination of the two opposite faces of the sample. Such arrangement made it possible to perform measurements either in forward- or in backscattering geometry. The 676.4-nm line of a cw krypton laser was chosen for the excitation. The corresponding photon energy, 1832 meV, was smaller by 50 meV than that of a luminescence maximum of the studied sample. An 0.85-m dual-grating monochromator, equipped with a cooled GaAs photomultiplier and an automated acquisition data system, was used to analyze the Raman-scattered radiation. The magnetic field was applied in the direction parallel to the sample surface and thus perpendicular to the c axis of the crystal. This was necessary to satisfy the light-scattering selection rules.^{17,27} The temperature was monitored by a calibrated carbon resistor located in close proximity to the sample. A strong sensitivity of Stokes shift at a given magnetic field upon the sample temperature was used to

determine an optimum excitation power, which on the one hand gave a reasonable signal-to-noise ratio, and on the other did not cause excessive heating of the sample. Such optimal power corresponded to the maximum power below which the Stokes shift became relatively power independent. Of course, since the thermal boundary resistance between the sample and surrounding liquid grows upon cooling, the optimal power decreases with decreasing temperature. Therefore, our dilution-refrigerator measurements at the lowest temperature were carried out with such a laser power on the sample (50–100 μW) that ensured that after a few hours scan time an adequate signal-to-noise ratio was obtained at the expense of some overheating. In order to reliably estimate sample temperature under these conditions, a sample with electrical contacts was immersed in the dilution refrigerator. By measuring sample resistance with and without laser illumination, we estimated that during the SFRS experiments the lowest sample temperature was $0.25 \pm 0.05 \text{ K}$. At the same time the temperature of the ^3He - ^4He mixture was as low as 0.1 K, while its value with the laser off dropped down to 0.05 K.

III. RESULTS AND DISCUSSION

A. Spin-flip Raman scattering spectra

Figure 1 shows examples of the Stokes-shift spectra, which we have attributed to the electron spin-flip transitions. Since the excitation power had to be reduced when the temperature was lowered, the intensity of scattered radiation diminished accordingly. It is seen in Fig. 1(b) that the Stokes-shift maximum at a given magnetic field increases with decreasing temperature, and in Fig. 1(c) at a given temperature it increases with the magnetic field. The Stokes shift of $\sim 3 \text{ meV}$ at 0.25 K and 1 kOe points to an effective Landé factor \bar{g} as large as 500. This directly confirms a dramatic influence of the s - d exchange interaction upon the spin splitting of electronic states.

By comparing results displayed in Fig. 1 with those for bound^{15–21} and itinerant^{27,28} electrons, we note several features of the spectra which demonstrate that itinerant electrons are being probed. First, the linewidth in Fig. 1(a) is larger in the backscattering geometry (open circles), consistent with a delocalized character of the spin states involved. Second, the line shape is Lorentzian, in contrast to the Gaussian line shape observed for bound electrons.^{15–20} In particular, at high temperatures ($T > 1 \text{ K}$), where the signal-to-noise ratio is the best, the fitting of the line by a Lorentzian function gives a mean-square deviation by at least a factor of 2 smaller than in the case of a Gaussian function. Finally, as illustrated in Fig. 1(c), the scattering intensity at constant laser power increases approximately linearly with the spin splitting in proportion to the excess number of spin-down electrons. This is again in contrast with SFRS spectra of bound electrons for which, once the BMP polarization vector becomes parallel to the magnetic field, the scattering intensity becomes field independent. Since the polaron magnetic moment^{17–19} is large, $\sim \frac{1}{2}\bar{g}\mu_B$, the alignment of the polaron quantization axes takes place at rather small magnetic

fields $\tilde{g}\mu_B H \leq k_B T$. (At very low temperatures, this alignment probably occurs for $\tilde{g}\mu_B H$ of the order of the anisotropy energy or characteristic energy of exchange interactions between neighboring donor electrons.)

As mentioned previously, the SFRS spectrum is proportional to a spin-spin correlation function. Thus, for itinerant electrons characterized by spin-splitting ω_s , spin-diffusion coefficient D_s , and spin-relaxation time T_2 ,

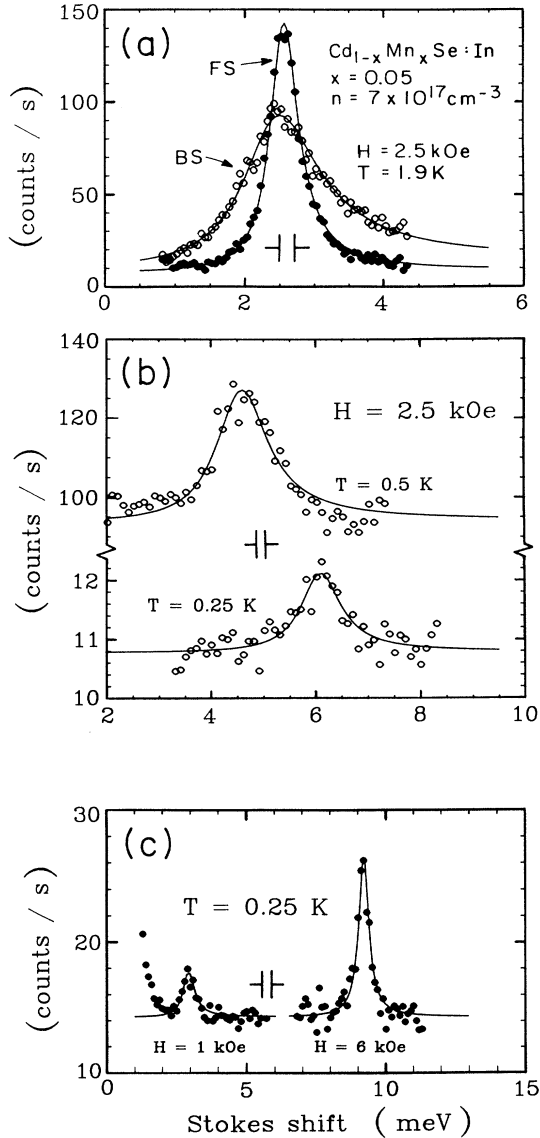


FIG. 1. Spin-flip Raman spectra of itinerant electrons in $\text{Cd}_{1-x}\text{Mn}_x\text{Se}:\text{In}$, $x=0.05$, $n=7 \times 10^{17} \text{ cm}^{-3}$, with solid curves showing fits to Eq. (1). The solid circles represent experimental data for forward scattering ($q \sim 0$), and open circles are for backscattering ($q = 5 \times 10^5 \text{ cm}^{-1}$). The temperature dependence is shown in (b) for $H=2.5 \text{ kOe}$. The magnetic field dependence is shown in (c) for $T=0.25 \text{ K}$. All spectra were taken with 1.832 eV laser excitation, and the instrumental resolution is illustrated by the vertical bars.

the SFRS intensity as a function of the frequency shift ω and scattering wave vector q assumes the form^{26,32-34}

$$S(\omega, \mathbf{q}) \propto \frac{G(1+F/2)}{1 + \exp(-\hbar\omega/k_B T)} \left[\frac{\omega\Gamma}{\Gamma^2 + (\omega - \omega_s)^2} + \frac{\omega\Gamma}{\Gamma^2 + (\omega + \omega_s)^2} \right], \quad (1a)$$

with

$$\Gamma = D_s q^2 + 1/T_2. \quad (1b)$$

Here, G is the thermodynamic density-of-states at the Fermi energy ϵ_F , and $1+F/2$ is an enhancement factor arising from the effects of electron-electron interactions. The same factor renormalizes both ω and ω_s (inside the large parentheses), but in order to conserve the standard form of the response function it has been absorbed into the definition of Γ .^{33,34} Expression (1) should be valid for $\hbar\omega_s \ll \epsilon_F$ as well as in the hydrodynamic limit, i.e., $\omega \ll 1/\tau$ and $\Gamma \ll 1/\tau$, where τ is the momentum relaxation time. The above inequalities are fulfilled in our case because $\hbar\tau \sim \epsilon_F \approx 20 \text{ meV}$, as estimated from the electron concentration $n = 7 \times 10^{17} \text{ cm}^{-3}$, conductivity $\sigma = 30 (\Omega \text{ cm})^{-1}$, and electron effective mass $m^*/m_0 = 0.13$.

Formula (1) was fit to experimental spectra treating ω_s and Γ , together with a proportionality factor and background intensity, as adjustable parameters (solid lines in Fig. 1). Having Γ for both $q \cong 0$ (forward-scattering geometry) and for $q = 5 \times 10^5 \text{ cm}^{-1}$ (backscattering geometry), T_2 and D_s were evaluated, taking into account corrections for the instrumental linewidth. The values of ω_s , T_2 , and D_s obtained in this way are discussed in subsequent sections. Before presenting this data, three additional remarks are in order. First, because of the ω factor in the numerator of Eq. (1a), the fitted values of ω_s are slightly smaller than positions of the Stokes-shift maxima ω_m . In particular, if $\hbar\omega_m \gg k_B T$, then $\omega_s = (\omega_m^2 - \Gamma^2)^{1/2}$. This demonstrates once again that a proper determination from spectroscopic studies of the energy of an elementary excitation requires knowledge of the response function of the system. Second, while SFRS experiments provide rather accurate information on ω_m and thus on ω_s , the values of Γ could be affected by several extrinsic effects. In particular, an inhomogeneous broadening of the line may arise from, for instance, from macroscopic inhomogeneities in the crystal composition or temperature gradients. Such effects will tend to diminish the measured values of T_2 but will cancel when determining D_s . Furthermore, an additional uncertainty in the determination of T_2 and D_s may be brought about by parasitic reflected laser light, which could perturb the purity of the scattering geometry. It is easy to see that the latter effect will diminish the apparent values of both T_2 and D_s . The above indicates that, strictly speaking, SFRS measurements provide a lower bound for the intrinsic values of T_2 and D_s . Third, our discussion will be based on the assumption that ω_s is determined by the mean-field part of the s - d interaction, while the difference between exact and mean-field s - d Hamiltonian will be treated only as a

source of electron scattering (which makes T_2 finite). Such an approach (adiabatic approximation) disregards dynamic aspects of the s - d coupling, i.e., effects of the coupling on the real part of electron self-energy. Because of the nonzero instrumental spectral width and a decrease of the Raman scattering intensity for $\omega \rightarrow 0$, we were able to probe only quasiparticles with relatively large energies $\omega \sim \omega_s \geq 1$ meV. Such energies are comparable to, or even greater than the width of the excitation spectrum of the interacting Mn subsystem in diluted magnetic semiconductors. It is plausible, therefore, that under our experimental conditions dynamic effects have not renormalized significantly the parameters of the response function.

B. Spin-splitting

Within the mean-field approximation ω_s is determined by a macroscopic magnetization M according to

$$\hbar\omega_s(T, H) = \frac{\alpha}{g\mu_B} M(T, H) + g^* \mu_B H, \quad (2)$$

where $\alpha N_0 = 0.28$ eV (Ref. 18) is the (ferromagnetic) s - d exchange energy; N_0 is the cation concentration; $g = 2.0$ and $g^* = 0.5$ are the Landé factors of Mn d electrons and band electrons in CdSe, respectively. In general, if localized and delocalized electrons coexist $M(T, H)$ may consist of two terms. The first of these is the background magnetization of Mn spins, possibly enhanced by the RKKY-type interaction. The Mn-based diluted magnetic semiconductors this part of M can be parametrized by a modified Brillouin function $B_{5/2}(T, H)$ for the spin $S = \frac{5}{2}$ of Mn^{2+} ions. The second part of M is brought about by magnetic moments of BMP's. In the magnetic field of interest these moments are already aligned, and thus to a good approximation, produce a field-independent contribution, $\hbar\omega_s^{(0)}(T)$. Hence, Eq. (2) can be rewritten in the form

$$\hbar\omega_s(T, H) = [\bar{g}(T) f_{5/2}(T, H) + g^*] \mu_B H + \hbar\omega_s^{(0)}(T). \quad (3)$$

Here,

$$\bar{g}(T) = \frac{\alpha \chi(T)}{g\mu_B^2} \quad (4)$$

is the effective Landé factor arising from the s - d exchange interaction, $\chi(T)$ is the zero-field magnetic susceptibility, and

$$f_s(y) = 3B_s(y) / [(S+1)y], \quad (5)$$

with

$$y = g\mu_B H / [k_B(T + T_0)], \quad (6)$$

where $T_0 = T_0(T)$ accounts for distant-neighbor interactions between Mn spins, including those mediated by itinerant electrons. Since a mean magnetic moment associated with each BMP is $\frac{1}{2} \bar{g} \mu_B$, the spin-splitting offset $\hbar\omega_s^{(0)}(T)$ takes the form

$$\hbar\omega_s^{(0)}(T) = N_p \alpha \bar{g}(T) / 2g, \quad (7)$$

where N_p is the concentration of those BMP's which are visited by itinerant electrons. It is interesting to note that if N_p is equal to the total BMP concentration, $M(T, H)$ in Eq. (2) corresponds to the macroscopic magnetization M_m , as given by direct magnetic measurements on the same sample [apart from a small diamagnetic correction and a paramagnetic correction involving g^* , not $\bar{g}(T)$]. This is in contrast to the case of localized electrons whose spin splitting is determined by a local magnetization, in general greater than the mean magnetization M_m .

As a first step, we fit the experimental values of ω_s to Eq. (3), treating $\bar{g}(T)$ and $T_0(T)$ as adjustable parameters and putting $\omega_s^{(0)}(T) \equiv 0$ (solid lines in Fig. 2). Results of the fitting procedure with $\omega_s^{(0)}(T)$ as an additional free parameter are shown by dashed lines on the same plot. The evaluated values of $\bar{g}(T)$ in these two ways are displayed as a function of temperature in Fig. 3. In order to compare this data with theoretical predictions of Eq. (3), we note that magnetic susceptibility measurements on a similar sample had been carried out.²³ These studies show that over the temperature range of interest, $\chi(T)$ (in emu) is well approximated by

$$\chi(T) = 1.8 \times 10^{-3} [T(K)]^{-0.62}. \quad (8)$$

Taking these values of $\chi(T)$ we get $\bar{g}(T)$, as shown by the straight line in Fig. 3. Since this curve does not involve any fitting parameter, the agreement between experimental and theoretical results is quite satisfactory. This agreement proves once more that the mean-field approximation accurately describes the s - d exchange interaction when dealing with electrons associated with a wide band. Furthermore, the above agreement confirms the known fact that electron-electron interactions [neglected in Eq. (3) for ω_s] do not affect the spin-resonance frequency, as

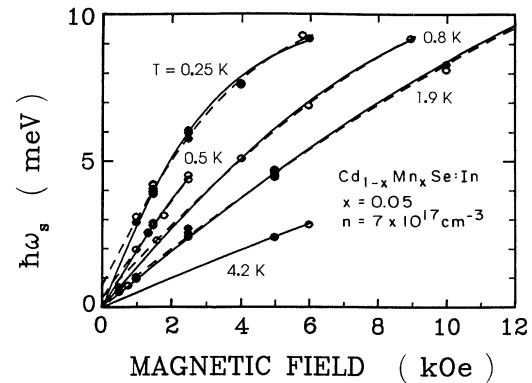


FIG. 2. Temperature dependence of the Stokes energy shift vs applied magnetic field obtained using spin-flip Raman scattering from itinerant electrons in $\text{Cd}_{1-x}\text{Mn}_x\text{Se}:\text{In}$, $x = 0.05$, $n = 7 \times 10^{17} \text{ cm}^{-3}$. Values for $\hbar\omega_s$ were obtained by fitting spectral data to Eq. (1). The open circles are for forward scattering, the solid circles are for backscattering. The curves show fits to Eq. (3) neglecting (solid lines) and taking into account a field-independent BMP energy (dashed curves).

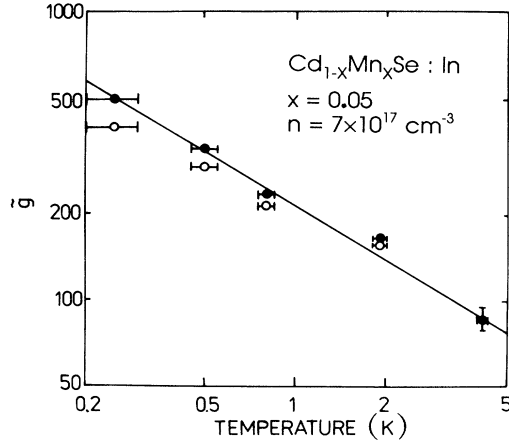


FIG. 3. Exchange-enhanced Landé g factor vs temperature for itinerant electrons in $\text{Cd}_{1-x}\text{Mn}_x\text{Se}:\text{In}$, $x=0.05$, $n=7\times 10^{17}\text{ cm}^{-3}$. Results were obtained from the fits in Fig. 2 neglecting (solid circles) and taking into account (open circles) a field-independent BMP energy. The solid line represents $\bar{g}(T)$ expected for a previously measured $\chi(T)$, with no adjustable parameters [Eq. (4)].

expected from Kohn's theorem. Putting this in a more general perspective, we note that the exchange interactions between electrons of the probed system (in our case Fermi-liquid electrons) do not affect the spin-resonance frequency. At the same time, the exchange coupling to an external system (in our case d electrons) does influence this frequency. We shall return to this problem later on.

We now turn to the spin-splitting offset $\hbar\omega_s^{(0)}(T)$. Its value obtained from the fit to the data increases from $\hbar\omega_s^{(0)}=0.1\pm 0.2\text{ meV}$ at 1.9 K to $\hbar\omega_s^{(0)}=0.6\pm 0.2\text{ meV}$ at 0.25 K. Assuming $N_p=3\times 10^{17}\text{ cm}^{-3}$, from Eq. (7) we also get $0.2\text{ meV}\leq \hbar\omega_s^{(0)}\leq 0.6\text{ meV}$ in the same temperature range. We conclude that our results concerning $\hbar\omega_s(T, H)$ are consistent with the conjecture about the existence of BMP's, and thus leads to the identification of local electron moments on the metallic side of the MIT. A question arises, however, why SFRS of BMP's were not seen directly in our study, particularly in the low field-region, where the efficiency of light scattering by itinerant electrons is small. A half-day of data collection showed no discernable BMP peak. It is probable that this negative result reflects the disappearance in the metallic phase of bound exciton states, which are known to constitute intermediate states for the SFRS involving localized electrons.

C. Spin-relaxation time

The dependence of T_2 on $\hbar\omega_s$ is shown in Fig. 4 for two different temperatures. The data at 1.9 K were taken up to 80 kOe, where $\hbar\omega_s\approx 19\text{ meV}$. In general, T_2 appears to be determined by two effects: a spin-orbit coupling and the s - d exchange interaction. A comparison of our T_2 values to those resulting from the SFRS measurements on nonmagnetic $\text{CdS}:\text{In}$ ²⁷ demonstrates that the

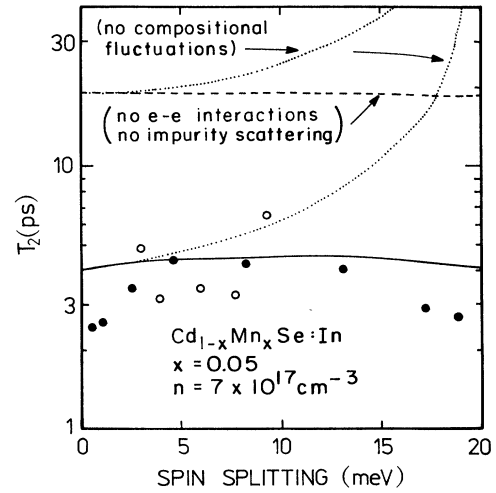


FIG. 4. Spin-relaxation time vs spin-split energy for itinerant electrons, obtained by comparing forward and backward spin-flip Raman scattering in $\text{Cd}_{1-x}\text{Mn}_x\text{Se}:\text{In}$, $x=0.05$, $n=7\times 10^{17}\text{ cm}^{-3}$. Solid (open) circles represent data for $T=1.9$ (0.25) K. The solid curve, from Eqs. (9), (17), and (18), represents scattering from fluctuations of magnetization, including the enhancements due to electron-electron interactions and localization from nonmagnetic scattering. [The dashed curve, Eqs. (9)–(14), ignores these enhancements.] The dotted curves show the effect when compositional fluctuations are ignored.

spin-orbit coupling gives a negligible contribution. The same conclusion stems from a previous evaluation of the spin-orbit relaxation rate for $\text{Cd}_{1-x}\text{Mn}_x\text{Se}:\text{In}$.²⁵ Thus, assuming the s - d interaction to be the dominant spin relaxation mechanism we have

$$1/T_2 = 2/\tau_{sx} + 2/\tau_{sz}, \quad (9)$$

where $1/\tau_{sx}$ is the scattering rate involving off-diagonal component of the s - d exchange Hamiltonian, $\sim \sum_i s_x S_x^{(i)}$, while $1/\tau_{sz}$ is determined by the difference between the diagonal part of the s - d Hamiltonian and its mean-field form. It is convenient to separate three scattering channels that can contribute to $1/\tau_{si}$ in the paramagnetic phase: (i) thermodynamic fluctuations of magnetization; (ii) statistical fluctuations in the distribution of magnetic ions in the random alloy (compositional fluctuations); (iii) randomly distributed ferromagnetic clouds of Mn spin around local electron moments (i.e., BMP's). As a first step we neglect electron scattering by BMP's. Furthermore, we disregard effects of electron-electron interactions and assume itinerant electrons to be described by plane waves. Following a standard procedure³⁵ we get

$$\frac{1}{\tau_{sx}^{(0)}} = \frac{k_F m^*}{4\pi\hbar^3} \frac{\alpha^2 k_B T}{g^2 \mu_B^2} \tilde{\chi}_1(T, H) \quad (10)$$

and

$$\frac{1}{\tau_{sz}^{(0)}} = \frac{k_F m^*}{4\pi\hbar^3} \left[\frac{\alpha^2 k_B T}{g^2 \mu_B^2} \tilde{\chi}_{\parallel}(T, H) + \frac{x(1-x)}{N_0} \left| \frac{d\hbar\omega_s(x)}{dx} \right|^2 \right], \quad (11)$$

where the second term in Eq. (11) arises from compositional fluctuations, with x denoting Mn content in the alloy. In general, $\chi_{\perp, \parallel}(T, H)$ in the above equations depend on the energy ε of quasiparticles that take part in the SFRS process (in our case $\varepsilon \leq \hbar\omega_s$). This dependence reflects the fact that taking interactions among Mn spins into account, the s - d scattering is inelastic. For $k_B T \ll \varepsilon$ we obtain

$$\tilde{\chi}_{\perp, \parallel}(T, H) \cong \frac{\beta}{\pi} \int \frac{\chi''_{xx, zz}(\omega') d\omega'}{1 - \exp(-\beta\omega')}, \quad (12)$$

where $\beta = \hbar/k_B T$. In the opposite limit, $k_B T \gg \varepsilon$, we have

$$\tilde{\chi}_{\perp, \parallel}(T, H) \cong \frac{\beta^2}{\pi} \int \frac{\omega' \chi''_{xx, zz}(\omega') d\omega'}{[\exp(\beta\omega') - 1][1 - \exp(-\beta\omega')]} . \quad (13)$$

Here $\chi''_{xx}(\omega)$ and $\chi''_{zz}(\omega)$ denote, respectively, the transverse and longitudinal imaginary parts of the Mn-spin dynamic susceptibility for $q \leq 2k_F$. If the energetic width of the Mn-spin excitation spectrum in the above q -range is smaller than $k_B T$, the denominators of Eqs. (12) and (13) can be expanded to lowest order $\beta\omega$. In this high-temperature case $\tilde{\chi}_{\perp, \parallel}(T, H)$ reduce, via the Kramers-Kronig relation, to the transverse and longitudinal static susceptibilities according to

$$\frac{1}{\tau_{pz}^{(0)}} = \frac{m^* k_F}{3\pi\hbar^3} \left[\frac{\alpha}{2g\mu_B} \right]^4 \chi_{\parallel}^2(T, H) \frac{N_p}{(k_F a_B)^2} \left[1 - \frac{1}{[1 + (k_F a_B)^2]^3} \right]. \quad (16)$$

This formula gives $T_{2p} = \tau_{pz}^{(0)}/2 \leq 240$ ps for $N_p = 3 \times 10^{17}$ cm⁻³ at $T = 1.9$ K. In view of this small scattering rate we next examine how $1/T_2$ is enhanced by electron-electron interactions^{34,36} and by localization effects, that is, by nonmagnetic impurity scattering.³⁶

In order to visualize how electron-electron interactions contribute to T_2 we note that the molecular field produced by Mn spins induces a spin-dependent redistribution of quasiparticles. The exchange interaction of an electron with Mn spins is, therefore, accompanied by an exchange interaction with the spin-polarized quasiparticles. This additional exchange interaction leaves, however, the electron-spin-resonance frequency intact. This is a well-known fact, which occurs because in the response function of Eq. (1), both ω_s and ω are renormalized by the interactions in the same way. Now, since the corresponding renormalization factor, $1 + F/2$, is absorbed into the definition of Γ it causes a reduction in the mea-

$$\tilde{\chi}_{\perp}(T, H) \cong \chi_{\perp}(T, H) \equiv M(T, H)/H, \quad (14a)$$

$$\tilde{\chi}_{\parallel}(T, H) \cong \chi_{\parallel}(T, H) \equiv \partial M(T, H)/\partial H. \quad (14b)$$

Since no detailed information of $\chi''_{xx, zz}(\omega)$ is available, we shall use the above high-temperature approximation in our quantitative calculations. In the case of $\tilde{\chi}_{\perp}$ this approximation certainly breaks down in extremely high magnetic fields $g\mu_B H \gg k_B T$, as $\chi_{xx}(\omega)$ has a strong maximum at the EPR frequency $\hbar\omega = g\mu_B H^*$, where H^* is the sum of the external field and the molecular field of electrons. There exists an indirect argument which supports the validity of the high-temperature approximation in the low-field region: it can be shown that the BMP energy is proportional to $\tilde{\chi}(T)$ as given by Eq. (12) rather than to the static susceptibility of Eq. (14). Analysis of the measured BMP energy down to 0.13 K suggests a numerical accord between these quantities.¹⁶

We have evaluated T_2 at 1.9 K from Eqs. (9)–(11) and (14). The results are shown as a dashed curve in Fig. 4. We see that the calculation misses an important ingredient. We therefore take into account spin-disorder scattering by BMP's. First, we consider the range of magnetic fields in which polarons are already aligned. In such a case a BMP located at \mathbf{R}_i and characterized by the localization radius a_B produces an additional magnetization of the form^{18,19}

$$\mathbf{M}(\mathbf{r}) = \frac{\alpha \chi_{\parallel}(T, H)}{2\pi a_B^3 g\mu_B} \exp(-2|\mathbf{r} - \mathbf{R}_i|/a_B), \quad (15)$$

where \mathbf{M} is directed along the magnetic field. We might regard BMP's as a source of an additional spin-dependent potential, which elastically scatter the itinerant electrons. Within the first Born approximation we get

measured values of both D_s and $1/T_2$. In addition, the exchange interaction of the electron with the spin-polarized quasiparticles affects the spin-relaxation rate $1/T_2$ directly, and is proportional to the mean square of the random molecular field experienced by the electron. In the static and long wavelength limits, this quasiparticle redistribution enhances $1/T_2$ by $(1 + F/2)^2$. Finally, taking these two contributions into account, the net effect of electron-electron interactions is to increase $1/T_2$ by $1 + F/2$.

Another correction to T_2 arises from electron scattering by nonmagnetic impurities. Such scattering allows the diffusing electron to return to the starting point and thus interact with a given Mn spin several times. If successive interaction events occur within the phase coherence time, the individual acts of scattering by the Mn ion cannot be regarded as independent. This leads to an enhancement of the cross section, and thus of $1/T_2$ by interference terms absent in the case of ballistic motion of

electrons.

We have evaluated the influence of the above two effects on T_2 , expressing the spin-disorder relaxation rate in terms of spin-spin correlation functions of the Mn and itinerant spin subsystems. The correlation functions can be related, in turn, to the q -dependent dynamic magnetic susceptibilities of Mn spins and electrons, respectively. Assuming that the hydrodynamic description of the electron liquid holds up to $q = \sqrt{3}l^{-1}$, where l is the mean-free path for elastic collisions, the scattering rate for thermodynamic and compositional fluctuations is expressed as

$$\frac{1}{\tau_{sx}} = \frac{(1+F/2)}{\tau_{sx}^{(0)}} \left[1 + \frac{3\sqrt{3}}{\pi(k_F l)^2} \left(1 - \frac{\pi}{2\sqrt{2}} \sqrt{\omega_s \tau} \right) \right], \quad (17)$$

$$\frac{1}{\tau_{sz}} = \frac{(1+F/2)}{\tau_{sz}^{(0)}} \left[1 + \frac{3\sqrt{3}}{\pi(k_F l)^2} \right], \quad (18)$$

where $\tau_{sx}^{(0)}$ and $\tau_{sz}^{(0)}$ are given in Eqs. (10) and (11).

In order to carry out a quantitative calculation of T_2 we take $l = 4.8 \times 10^{-7}$ cm and $\tau = 2.0 \times 10^{-14}$ s, as given by conductivity $\sigma = 30$ ($\Omega \text{ cm}$) $^{-1}$, and electron concentration $n = 7 \times 10^{17}$ cm $^{-3}$. Furthermore, we adopt $F = 3$, a value deduced from previous studies of the spin-splitting-induced magnetoresistance in similar samples of Cd $_{0.95}$ Mn $_{0.05}$ Se:In.²³ The results of the calculation are shown for 1.9 K by the solid curve in Fig. 4. We see that the present theory, with no adjustable parameters, describes correctly the experimental results.

We have also calculated T_2 neglecting compositional fluctuations of magnetization, as shown by the dotted curves in Fig. 4. The results demonstrate that compositional fluctuations constitute the main mechanism of the line broadening in the high-field region.

Electron-electron interactions as well as scattering by nonmagnetic impurities may also affect the efficiency of scattering by BMP's. Actually, the corresponding enhancement factor is relatively large, as magnetization produced by BMP's varies slowly in space. The polaron-limited relaxation time is evaluated to be

$$\frac{1}{T_{2p}} = \frac{2(1+F/2)}{\tau_{pz}^{(0)}} \left[1 + \frac{3\sqrt{3}}{\pi(k_F l)^2} (1 + k_F^2 a_B^2) \right], \quad (19)$$

where $\tau_{pz}^{(0)}$ is given by Eq. (16). The above formula implies that T_{2p} would be as long as 32 ps at 1.9 K, for $H \rightarrow 0$, and $N_p = 3 \times 10^{17}$ cm $^{-3}$. The polaron scattering may, however, dominate at lower temperatures. This is because the efficiency of scattering by thermodynamic fluctuations [proportional to $T\chi(T)$] decreases with decreasing temperature while the efficiency of scattering by BMP's [proportional to $\chi^2(T)$] increases sharply when the temperature is lowered. For the sample under consideration we have from Eq. (19) $T_{2p} \approx 2.5$ ps at 0.25 K and for $H \rightarrow 0$, a value about four times smaller than the expected relaxation time due to scattering by thermodynamic fluctuations [Eqs. (9), (17), and (18)]. Unequivocal experimental information on scattering by polarons would require accurate linewidth measurements at lower

temperatures and smaller magnetic fields than those at which we were able to detect the SFRS signal.

D. Spin-diffusion coefficient

In addition to the spin-splitting and spin-relaxation time, our SFRS experiments have provided some information on spin-diffusion processes. As shown in Fig. 5, the spin-diffusion coefficient D_s at 1.9 K, estimated from the SFRS linewidth, falls in the range 2–4 cm 2 /s. *A priori*, spin diffusion may proceed via charge transport or exchange interactions among electrons. In the former case D_s is related to the conductivity σ according to the Einstein relation

$$D_s = \frac{\pi^2 \hbar^2 \sigma}{(1+F/2)e^2 m^* k_F}, \quad (20)$$

where a reduction of D_s by the electron-electron interaction has been taken into account following arguments presented in the previous section. Taking material parameters suitable for our sample, we get $D_s \approx 2$ cm 2 /s. This number is in agreement with the measured values, indicating that the spin diffusion is mostly caused by charge transport, as could be expected for delocalized electrons.

Earlier transport studies of n -type Cd $_{1-x}$ Mn $_x$ Se near the metal-to-insulator transition^{3,23–25} have revealed a large positive magnetoresistance. This magnetoresistance was shown to arise from the influence of the spin splitting upon quantum corrections to the conductivity.²⁵ More precisely, the spin splitting strongly affects scattering-

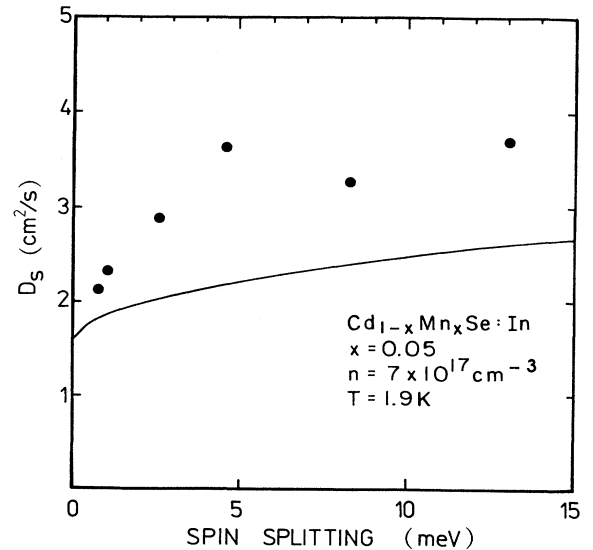


FIG. 5. Spin diffusion coefficient vs spin splitting for itinerant electrons, obtained by comparing forward and backward spin-flip Raman scattering in Cd $_{1-x}$ Mn $_x$ Se:In, $x = 0.05$, $n = 7 \times 10^{17}$ cm $^{-3}$. The solid points represent data for $T = 1.9$ K. The solid curve shows the frequency-dependent diffusion arising from the influence of localization corrections that result from interference of scattered waves, given by Eq. (21).

modified electron-electron interactions but has a negligible influence on that localization correction which results from interference of scattered waves.⁵ The positive magnetoresistance implies, via the Einstein relation, a decrease of D_s with the increasing magnetic field. This expectation is at variance with the experimental results of Fig. 5, which point to an increase of D_s with the spin splitting. We assign this apparent inconsistency to the fact that in contrast to d.c. transport measurements, the SFRS experiment determines the diffusion coefficient at nonzero frequency, $\omega \approx \omega_s$. Actually, it is known⁵ that the magnitude of the quantum corrections decreases when the frequency increases. At the same time, the diffusion coefficient is expected to acquire an imaginary part, $D_s''(\omega)$. In the case of the correction caused by the interference, the frequency dependence of the diffusion coefficient is given by⁵

$$D_s(\omega) = D_s(0) \left[1 + \frac{3\sqrt{3}}{2\sqrt{2}} \frac{\sqrt{\omega\tau}}{(k_{Fl})^2} (1-i) \right]. \quad (21)$$

The real part of $D_s(\omega)$, calculated for $\omega = \omega_s$, is plotted as a solid curve in Fig. 5. We conclude that the effect in question is responsible, at least partly, for the dependence of D_s on ω_s .

Still another role is played by the imaginary part of $D_s(\omega)$. It is easy to show that $D_s''(\omega)$ induces a shift of the resonance frequency according to $\omega_s \rightarrow \omega_s + D_s''(\omega)q^2$. If indeed, as Eq. (21) suggests, $D_s''(\omega) < 0$, we may expect ω_s determined in the forward-scattering geometry ($q=0$) to be greater than ω_s determined from the backscattering spectra. Experimental results summarized in Figs. 1(a) and 2 tend to confirm this expectation.

An additional dependence of D_s on ω_s , qualitatively similar to that of Eq. (21), will presumably result from effects of scattering on electron-electron interactions. While an exact formula has to be worked out, it appears that a correction to Eq. (21) should be small, as the contribution from electron-electron interactions is described by two terms of a similar magnitude but opposite sign.⁵

IV. CONCLUSIONS

Our work has demonstrated the feasibility of probing band electrons by means of inelastic light scattering at subkelvin temperatures. Such studies are particularly rewarding in diluted magnetic semiconductors because of strong variations of material properties with temperature. We have found, in particular, that in the case of n -type $\text{Cd}_{0.95}\text{Mn}_{0.05}\text{Se}$ the Stokes shift associated with the elec-

tron spin-splitting increases sharply with decreasing temperature to attain at 0.25 K a value which corresponds to an effective Landé factor as large as 500. A quantitative description of the spin splitting as a function of the temperature and magnetic field has confirmed the applicability of the mean-field approximation to the s - d exchange interaction when dealing with delocalized electrons in a wide conduction band. An accurate examination of the data in weak magnetic fields has shown, however, that the spin splitting tends to nonzero value for the vanishing magnetic field. This effect has been explained by us in terms of the two fluid models of electronic states near the metal-to-insulator transition. Within this model the zero-field spin splitting of itinerant electrons is induced by the permanent magnetization that exists inside the localization orbit of local s spins. A comparison of numerical estimates with experimental results has supported this interpretation.

Another piece of interesting information has emerged from our analysis of the line broadening mechanisms. In the forward-scattering geometry the linewidth appears to be determined by fluctuations of the Mn spin magnetization, the thermodynamic fluctuation giving the dominant contribution in weak magnetic fields, with the effect of random distribution of magnetic ions taking over in strong fields. The above broadening mechanism has turned out to be strongly enhanced by both electron-electron interactions and localization effects. The influence of the above effects has been particularly large under our experimental conditions because of the proximity to the metal-to-insulator transition. In the backscattering geometry the spin-diffusion processes contribute, making the linewidth larger. Again, the spin-diffusion coefficient has been shown to be affected by electron-electron interactions and localization corrections.

ACKNOWLEDGMENTS

The Francis Bitter National Magnet Laboratory is supported by the National Science Foundation through cooperative agreement DMR-8813164, and the present work was supported by NSF Grant No. DMR-8807419. The work at the Institute of Physics, Polish Academy of Sciences and travel grants were supported in part by the Institute for Low Temperatures and Structural Research, Polish Academy of Sciences, through Grant No. CPBR 15.6. We thank L. Rubin and B. Brandt of the FBNML, and B. Goldberg and J. Brooks of Boston University for their help.

¹For a review, see, e.g., *Anderson Localization*, edited by T. Ando and H. Fukuyama (Springer, Berlin, 1988).

²R. N. Bhatt, M. A. Paalanen, and S. Sachdev, *J. Phys.* **49-C8**, 1179 (1988), and references therein.

³T. Dietl, L. Swierkowski, J. Jaroszynski, M. Sawicki, and T. Wojtowicz, *Phys. Scr.* **T14**, 29 (1986).

⁴S. Sachdev, *Phys. Rev. B* **39**, 5297 (1989).

⁵See, e.g., B. L. Al'tshuler, A. G. Aronov, D. E. Khmel'nitskii,

and A. I. Larkin, in *Quantum Theory of Solids*, edited by I. M. Lifshits (Mir, Moscow, 1982), p. 130; P. A. Lee and T. V. Ramakrishnan, *Rev. Mod. Phys.* **57**, 287 (1984); B. L. Al'tshuler and A. G. Aronov, in *Electron-Electron Interactions in Disordered Systems*, edited by A. L. Efros and M. Pollak (North-Holland, Amsterdam, 1985), p. 1; H. Fukuyama, *ibid.*, p. 155; A. M. Finkel'stein, *Zh. Eksp. Teor. Fiz.* **86**, 367 (1984) [*Sov. Phys.—JETP* **59**, 212 (1984)]; C. Castellani, D.

- DiCastro, P. A. Lee, and M. Ma, *Phys. Rev. B* **30**, 527 (1984); C. Di Castro, in *Anderson Localization* (Ref. 1), p. 96; G. Kotliar, *ibid.*, p. 107; T. Dietl, M. Sawicki, J. Jaroszynski, T. Wojtowicz, W. Plesiewicz, and A. Lenard, in *Proceedings of the 19th International Conference on the Physics of Semiconductors, Warsaw, 1988*, edited by W. Zawadzki (Institute of Physics, Warsaw, 1988), p. 1189.
- ⁶M. Lakner and H. v. Lohneyson, *Phys. Rev. Lett.* **63**, 648 (1989).
- ⁷D. Romero, M.-W. Lee, H. D. Drew, M. Shayegan, and B. S. Elman, in *Anderson Localization* (Ref. 1), p. 53.
- ⁸H. Kamimura, *Philos. Mag.* **B52**, 541 (1985), and references therein; M. Eto, O. Sugino, and H. Kamimura, in *Proceedings of the 19th International Conference on the Physics of Semiconductors, Warsaw, 1988* (Ref. 5) p. 1213.
- ⁹M. Milovanovic, S. Sachdev, and R. N. Bhatt, *Phys. Rev. Lett.* **63**, 82 (1989).
- ¹⁰W. Wojtowicz, T. Dietl, M. Sawicki, W. Plesiewicz, and J. Jaroszynski, *Phys. Rev. Lett.* **56**, 2419 (1986).
- ¹¹Z. Wilamowski, K. Swiatek, T. Dietl, and J. Kossut, *Solid State Commun.* **74**, 833 (1990).
- ¹²J. Wróbel, T. Dietl, G. Karczewski, J. Jaroszynski, W. Plesiewicz, A. Lenard, M. Dybiec, and M. Sawicki, *Semicond. Sci. Technol.* **5**, S299 (1990).
- ¹³J. Jaroszynski, T. Dietl, M. Sawicki, T. Wojtowicz, and W. Plesiewicz, in *High Magnetic Fields in Semiconductor Physics II*, edited by G. Landwehr (Springer, Berlin, 1988), p. 514.
- ¹⁴Some of the results presented in this paper are briefly discussed, in E. D. Isaacs, T. Dietl, M. Sawicki, D. Heiman, M. Dahl, M. J. Graf, S. I. Gubarev, and D. L. Alov, *Proceedings of the 19th International Conference on Low Temperature Physics, Brighton, 1990* [*Physica B* **165&166**, 235 (1990)]; T. Dietl, M. Sawicki, E. D. Isaacs, M. Dahl, D. Heiman, M. J. Graf, S. I. Gubarev, and D. L. Alov, in *Proceedings of the 20th International Conference on the Physics of Semiconductors, Thessaloniki* (World Scientific, in press).
- ¹⁵M. Nawrocki, R. Planel, G. Fishman, and R. R. Galazka, *Phys. Rev. Lett.* **46**, 735 (1981); R. Planel, T. H. Nhung, G. Fishman, and M. Nawrocki, *J. Phys. (Paris)* **45**, 1071 (1984); D. L. Peterson, D. U. Bartholomew, U. Debska, A. K. Ramdas, and S. Rodriguez, *Phys. Rev. B* **32**, 323 (1985).
- ¹⁶E. D. Isaacs, D. Heiman, M. J. Graf, B. B. Goldberg, R. Kershaw, K. Dwight, A. Wold, J. K. Furdyna, and J. S. Brooks, *Phys. Rev. B* **37**, 7108 (1988).
- ¹⁷D. Heiman, P. A. Wolff, and J. Warnock, *Phys. Rev. B* **27**, 4848 (1983); E. D. Isaacs, D. Heiman, P. Becla, Y. Shapira, R. Kershaw, K. Dwight, and A. Wold, *ibid.* **38**, 8412 (1988).
- ¹⁸T. Dietl and J. Spalek, *Phys. Rev. Lett.* **48**, 355 (1982); *Phys. Rev. B* **28**, 1548 (1983).
- ¹⁹S. M. Ryabchenko and Yu G. Semenov, *Zh. Eksp. Teor. Fiz. [Sov. Phys.—JETP]* **57**, 825 (1983)].
- ²⁰T. Dietl, *J. Magn. Magn. Mater.* **38**, 34 (1983).
- ²¹Y. Shapira, D. Heiman, and S. Foner, *Solid State Commun.* **44**, 1243 (1982); D. Heiman, Y. Shapira, S. Foner, B. Khazai, R. Kershaw, K. Dwight, and A. Wold, *Phys. Rev. B* **29**, 5634 (1984).
- ²²M. A. Novak, O. G. Symko, D. J. Zheng, and S. Oseroff, *Phys. Rev. B* **33**, 6391 (1986).
- ²³T. Dietl, M. Sawicki, T. Wojtowicz, J. Jaroszynski, W. Plesiewicz, L. Swierkowski, and J. Kossut, in *Anderson Localization* (Ref. 1), p. 58.
- ²⁴Y. Shapira, D. H. Ridgley, K. Dwight, A. Wold, K. P. Martin, J. S. Brooks, and P. A. Lee, *Solid State Commun.* **54**, 593 (1985); Y. Shapira, N. F. Oliveira, D. H. Ridgley, R. Kershaw, K. Dwight, and A. Wold, *Phys. Rev. B* **34**, 4187 (1986).
- ²⁵M. Sawicki, T. Dietl, J. Kossut, J. Igalson, T. Wojtowicz, and W. Plesiewicz, *Phys. Rev. Lett.* **56**, 508 (1986).
- ²⁶P. A. Wolff, J. G. Ramos, and S. Yuen, in *Theory of Light Scattering in Condensed Matter*, edited by B. Bendow, J. L. Birman, and V. M. Agranovich (Plenum, New York, 1976), p. 475; P. A. Wolff, in *Diluted Magnetic Semiconductors, Semiconductors and Semimetals*, edited by J. K. Furdyna and J. Kossut (Academic, New York, 1988), Vol. 25, Chap. 10.
- ²⁷S. Geschwind and R. Romestain, in *Light Scattering in Solids IV*, edited by M. Cardona and G. Guntherodt (Springer, New York, 1978), p. 164.
- ²⁸D. L. Alov, G. I. Gubarev, and V. B. Timofeev, *Zh. Eksp. Teor. Fiz.* **86**, 1124 (1984) [*Sov. Phys.—JETP* **59**, 658 (1984)].
- ²⁹J. Warnock, D. Heiman, P. A. Wolff, R. Kershaw, D. Ridgley, A. Wold, and R. R. Galazka, in *Proceedings of the 17th International Conference on the Physics of Semiconductors*, edited by J. D. Chadi and W. A. Harrison (Springer, New York, 1985), p. 1405; J. A. Gaj, *ibid.*, p. 1423.
- ³⁰H. Krenn, W. Zawadzki, and G. Bauer, *Phys. Rev. Lett.* **55**, 1510 (1985); D. D. Awschalom, J. Warnock, and S. Von Molnar, *ibid.* **58**, 812 (1987); H. Krenn, K. Kaltenecker, T. Dietl, J. Spalek, and G. Bauer, *Phys. Rev. B* **39**, 10918 (1989).
- ³¹E. D. Isaacs and D. Heiman, *Rev. Sci. Instrum.* **58**, 1672 (1987); D. Heiman, X. L. Zheng, S. Sprunt, B. B. Goldberg, and E. D. Isaacs, *SPIE* **1055**, 96 (1989).
- ³²M. A. Garstens, L. S. Singer, and A. H. Ryan, *Phys. Rev.* **96**, 53 (1954).
- ³³P. Platzman and P. A. Wolff, *Phys. Rev. Lett.* **18**, 280 (1967).
- ³⁴A. M. Finkelstein, *J. Phys.* **49-C8**, 1170 (1988).
- ³⁵C. Haas, *Crit. Rev. Solid State Sci.* **1**, 47 (1970); K. H. Fischer, *Z. Phys. B* **34**, 45 (1979).
- ³⁶S. Sachdev, *Phys. Rev. B* **34**, 6049 (1986).